Electronic Supplementary Information to:

Enhanced photoresponse of large-sized photoactive graphene composite films based on water-soluble conjugated polymers

*Jinhua Sun, Linhong Xiao, Dongli Meng, Jianxin Geng,** and *Yong Huang*

Technical Institute of Physics and Chemistry, Chinese Academy of Sciences
29 Zhongguancun East Road, Haidian District, Beijing 100190 (China)
E-mail: jianxingeng@mail.ipc.ac.cn

S1. Synthesis of P3TOPS and P3TOPA

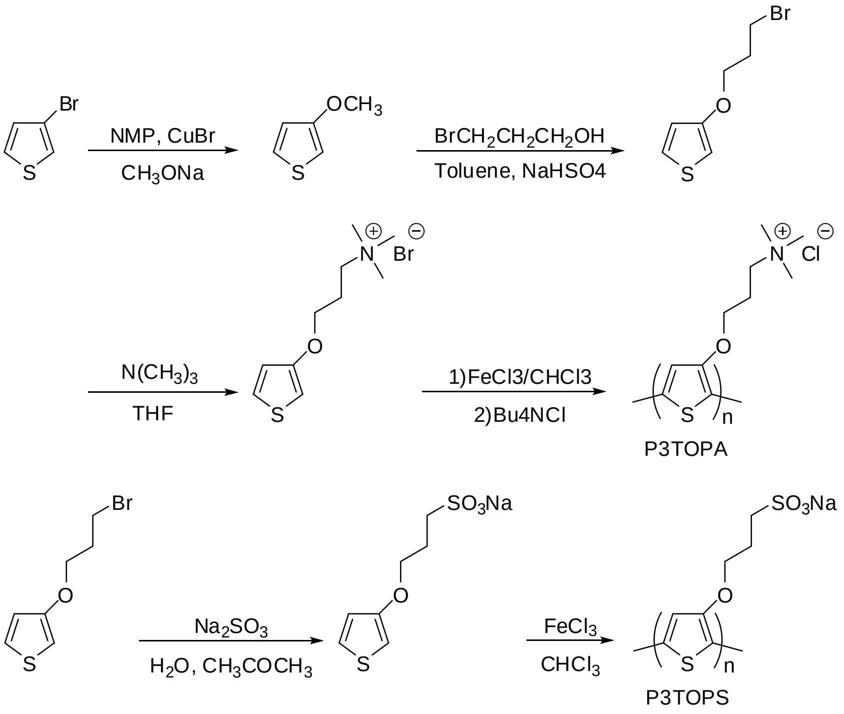

Scheme S1. Synthesis of P3TOPA and P3TOPS.

Synthesis of P3TOPS and P3TOPA was performed by following references.[1-2] In Scheme S1 is displayed the synthesis of P3TOPS and P3TOPA.

Synthesis of 3-methoxythiophene. 3-Methoxythiophene was synthesized by a nucleophilic substitution reaction on thiophene ring. In a typical reaction, 3-bromothiophene (5 g, 30.7 mmol) was added to a mixture of sodium methoxide (28% in methanol, 18 ml) and NMP (6.8 ml) under protection of Ar. After the solid was dissolved, CuBr (2.5 g, 17.4 mmol) was added into the solution. And then, the mixture was refluxed for 3 days in Ar atmosphere. After cooling, the reaction mixture was filtered and extracted with deionic (DI) water, and the water phase was extracted with diethyl ether for three times. The organic phase was collected and dried with anhydrous $MgSO_4$. The solvent was removed by rotary evaporation. The product was purified by silica column chromatography using hexane as eluent. Finally, 2.635 g product was obtained after the solvent was removed by rotary evaporation (yield 80.3%). ^{1}H NMR ($CDCl_3$, δ, ppm, TMS): 7.18 (1H, s, 2-position of thiophene ring), 6.74 (1H, d, 5-position of thiophene ring), 6.25 (1H, d, 4-position of thiophene ring), 3.81 (3H, s, $C_4H_3SOC\mathbf{H}_3$).

Synthesis of 3-(3-bromo)propoxythiophene. In a typical reaction, 3-methoxythiophene (2.86 g, 25.09 mmol), 3-bromo-1-propanol (7.67 g, 55.19 mmol), and $NaHSO_4$ (471.55 mg, 3.41 mmol) were added into toluene (46 mL) under Ar atmosphere, followed by refluxing at 100 °C for 6 h. Then the reaction mixture was cooled to room temperature and washed three times with DI water. The collected water phase was extracted with diethyl ether. The organic phases were combined and dried with anhyrous $MgSO_4$. Crude product was obtained by removing the solvent via rotary evaporation, and purified by silica column chromatography using hexane as eluent. A colorless oil was finally obtained after removing the solvent (2.0186 g, yield 67.1%). ^{1}H NMR ($CDCl_3$, δ, ppm, TMS): 7.17 (1H, s, 2-position of thiophene ring), 6.74 (1H, d, 5-position of thiophene ring), 6.27 (1H, d, 4-position of thiophene ring), 4.08 (2H, t, $C_4H_3SOC\mathbf{H}_2CH_2CH_2Br$), 3.58 (2H, t, $C_4H_3SOCH_2CH_2C\mathbf{H}_2Br$), 2.30 (2H, m, $C_4H_3SOCH_2C\mathbf{H}_2CH_2Br$).

Synthesis of 3-(3-thienyloxy)propyltrimethylammonium bromide. In a typical reaction, trimethylamine (30 mL, 50 wt% in water) was added into a solution of 3-(3-bromo)propoxythiophene (2.0186 g, 9.13 mmol) in THF (120 mL). The mixture was stirred for 24 h at room temperature. After that, crude product was obtained by removing the solvent using rotary evaporation. The crude product was washed with THF to give the purified product (1.058 g, 73.0%). ^{1}H NMR (D_2O, δ, ppm): 7.39 (1H, s, 2-position of thiophene ring), 6.86 (1H, d, 5-position of thiophene ring), 6.59 (1H, d, 4-position of thiophene ring), 4.19 (2H, t, $C_4H_3SOC\mathbf{H}_2CH_2CH_2N(CH_3)_3Br$), 3.56 (2H, t, $C_4H_3SOCH_2CH_2C\mathbf{H}_2N(CH_3)_3Br$), 3.17 (9H, s, $C_4H_3SOCH_2CH_2CH_2N(C\mathbf{H}_3)_3Br$), 2.30 (2H, m, $C_4H_3SOCH_2C\mathbf{H}_2CH_2N(CH_3)_3Br$).

Synthesis of P3TOPA. In a typical reaction, 3-(3-thienyloxy)propyltrimethylammonium bromide (270 mg, 0.96 mmol) and anhydrous $FeCl_3$ (590 mg, 3.63 mmol) were added to $CHCl_3$ (30 mL) under Ar atmosphere, followed by stirring for 24 hours at room temperature. After that, methanol (100 ml) was added to the mixture to stop the polymerization. Solid was obtained by filtration, and extracted by acetone/Soxhlet for 24 hours. And then, the insoluble fraction of the polymer was dissolved in methanol with a few drops of hydrazine. The polymer was precipitated by addition of a saturated tetrabutylammonium chloride solution in acetone to get the product, and further washed with acetone. The polymer was finally dried in vacuum (98.5 mg, 43.5%). ^1H NMR (D_2O, δ, ppm): 7.28 (1H, s, 4-position of thiophene ring), 4.42 (2H, t, $C_4HSOC\mathbf{H}_2CH_2CH_2N(CH_3)_3Cl$), 3.63 (2H, t, $C_4HSOCH_2CH_2C\mathbf{H}_2N(CH_3)_3Cl$), 3.20 (9H, s, $C_4HSOCH_2CH_2CH_2N(C\mathbf{H}_3)_3Cl$), 2.37 (2H, m, $C_4HSOCH_2C\mathbf{H}_2CH_2N(CH_3)_3Cl$).

Suntheis of sodium 3-(3-thienyloxy)propanesulfonate. In a typical reaction, 3-(3-bromo)propoxythiophene (0.5525 g, 2.5 mmol) and Na_2SO_3 (0.630 g, 5 mmol) were added into a mixture of DI water (5 ml) and acetone (10 ml), followed by refluxing for 48 hours. After cooling, the solution was washed with diethyl ether. The water phase was collected, and the water was removed by rotary evaporation. The crude product was dissolved in DI water, and the inorganic salt was precipitated by addition of a few drops of ethanol, and removed by filtration. 0.44 g product was obtained after the solvent was removed from the filtrate by rotary evaporation (yield 72%). ^1H NMR (D_2O, δ, ppm): 7.38(1H, s, 2-position of thiophene ring), 6.86 (1H, d, 5-position of thiophene ring), 6.60 (1H, d, 4-position of thiophene ring), 4.20 (2H, t, $C_4H_3SOC\mathbf{H}_2CH_2CH_2SO_3Na$), 3.09 (2H, t, $C_4H_3SOCH_2CH_2C\mathbf{H}_2SO_3Na$), 2.23 (2H, m, $C_4H_3SOCH_2C\mathbf{H}_2CH_2SO_3Na$).

Synthesis of P3TOPS. In a typical reaciton, sodium 3-(3-thienyloxy)propanesulfonate (458.2 mg, 1.88 mmol) and anhydrous $FeCl_3$ (2.43 g, 15.04 mmol) were added to $CHCl_3$ (50 ml) under Ar atmosphere, followed by stirring for 24 hours at room temperature. To stop the reaction, methanol (100 ml) with a few drops of hydrazine was added to the mixture. After that, the resulting polymer was precipitated in a 1 M NaOH solution in methanol (300 mL), and then washed with methanol. The product as dark powder was obtained after drying in vacuum (0.197 g, yield 43%). ^{1}H NMR (D_2O, δ, ppm): 7.05 (1H, s, 4-position of thiophene ring), 4.41 (2H, t, $C_4HSOC\mathbf{H}_2CH_2CH_2SO_3Na$), 3.23 (2H, t, $C_4HSOCH_2CH_2C\mathbf{H}_2SO_3Na$), 2.32 (2H, m, $C_4HSOCH_2C\mathbf{H}_2CH_2SO_3Na$).

S2. Characterization of CCG/P3TOPS suspension

The dispersibility of the CCG/P3TOPS sheets was characterized using AFM (Fig. S1). AFM observation revealed that there is no aggregation of the CCG/P3TOPS sheets in the films spin-coated on mica substrate, indicating high dispersibility of the CCG/P3TOPS sheets in the aqueous suspension. The CCG/P3TOPS sheets have size ranging from submicrons to microns. Cross-section analysis shows that the thickness of the CCG/P3TOPS sheets ranges from 1.5 to 2.3 nm, which is greater than the value of GO sheets (ca. 1 nm) due to the attachment of the P3TOPS chains on the surfaces of the CCG sheets.

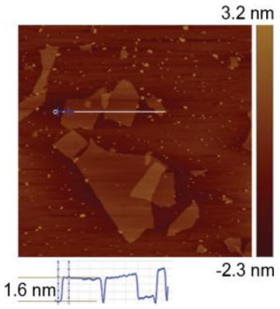

Figure S1. An AFM image of CCG/P3TOPS sheets coated on mica substrate (scanning area: 20×20 μm^2).

The reduction extent of the GO was characterized using UV-visible spectroscopy (Fig. S2a). The absorption spectrum of a P3TOPS solution shows an absorption maximum at 435 nm (the solid line). A GO suspension yields an absorption spectrum containing an absorption maximum at 230 nm (the dash-dot line). In contrast, the P3TOPS stabilized CCG suspension gives an absorption spectrum that contains an absorption maximum at 271 nm and markedly enhanced absorption in the whole visible range (the dash line). The red shift of the absorption maximum indicates the conversion of GO sheets to CCG sheets via chemical reduction by hydrazine.[3-5] In Fig. S2b are displayed the PL spectra of P3TOPS solution and the CCG/P3TOPS composite suspension, excited with a laser of wavelength 435 nm. A P3TOPS solution generates an emission peak at 518 nm (the solid line), whereas the PL of P3TOPS was completely quenched by the CCG sheets in the CCG/P3TOPS composite suspension. This result is due to the photoinduced electron transfer from P3TOPS to CCG sheets, indicating electron D-A properties of the CCG/P3TOPS composite.

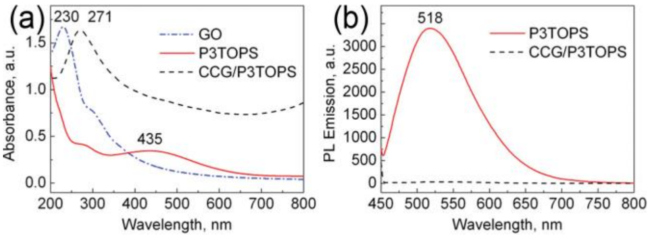

Figure S2. (a) UV-visible spectra of GO suspension, P3TOPS solution, and CCG/P3TOPS suspension in water; (b) PL spectra of P3TOPS solution and CCG/P3TOPS composite suspension in water.

S3. Preparation of CCG/P3TOPS-P3TOPA composite films and photoresponse devices

CCG/P3TOPS-P3TOPA composite films were prepared on glass, quatz, and SiO_2/Si wafer. The substrates were sequentially cleaned by sonication in ethanol, acetone, isopropyl alcohol, and DI water for 10 minutes in each solvent, and finally dried with N2 flow. Hydroxyl groups were further generated on the surfaces of the substrates. The cleaned substrates were sonicated in a piranha solution (concentrated H_2SO_4:H_2O_2 aqueous solution = 7:3) for 1 h, and further soaked in the piranha solution for one more hour. After that, the substrates were rinsed with DI water, and dried with N_2 flow.

In order to improve the affinity of the CCG/P3TOPS sheets to the substrates, the substrates were treated with PDDA.[6-7] This treatment was completed by soaking the substrates in a PDDA aqueoous sultion (1 wt%) for 5 min, and thereafter rinsing with DI water and drying with N_2 flow. To fulfill the layer-by-layer assembly, the PDDA-treated substrates was soaked in a CCG/P3TOPS suspension (0.25 $mg{\cdot}ml^{-1}$) for 10 min, rinsed with DI water, and dried with N_2 flow. And then, a P3TOPA layer was coated by using a P3TOPA solution (0.25 $mg{\cdot}ml^{-1}$), which contained Na_2SO_4 (0.2 M) for adjusting the ionic strength of the solution.[8] As a result, photoactive CCG/P3TOPS-P3TOPA composite films of various thickness were prepared by repeating the above operation. The films were designated as x-cycled CCG/P3TOPS-P3TOPA composite films (where x stands for the repeating times of the LBL cycle).

Photoresponse devices were prepared by coating two AL contacts (ca. 100 nm thick) on the CCG/P3TOPS-P3TOPA composite films using a mask to protect the active areas so that the devices have active areas of $10\times10\ mm^2$ (the inset of Fig. 3b). Finally, the devices were thermally annealed at 70 °C in vacuum for 60 min.

At first, I-V curves of the devices were measured in the dark. Since the area between the two electrodes is square ($10\times10\ mm^2$), the resistance of the films calculated from the I-V curves is sheet resistance.

Photocurrent response was measured by applying 1 V bias between the two contacts while the illuminaiton path was opened and chopped periodically. The intensity of illumination was fixed at 100 $mW{\cdot}cm^{-2}$ (AM 1.5) if not stated elsewhere. The illumination was produced using a CEL-HXB UV300 light source.

S4. Morphology of CCG/P3TOPS-P3TOPA composite films

In Fig. S3a is displayed a AFM image of CCG/P3TOPS sheets coated on poly(diallyldimethylammonium chloride) (PDDA) treated glass substrate by dip coating.[6-7] It's seen that the CCG/P3TOPS sheets dispersively distribute on the substrate. In Fig. S3b are shown needle-like microcrystals of P3TOPA dip-coated on glass substrate. Such morphology is similar to the single crystals of poly(3-hexylthiophene),[9-10] a typical conjugated polymer that has been widely used in organic optoelectronics. However, when coated on the surface of a CCG/P3TOPS composite layer, the P3TOPA does not show the clear needle-like microcrystals anymore (Fig. S3c). This finding might be due to the interactions between the CCG/P3TOPS sheets and P3TOPA molecules, which influence the crystallization of P3TOPA. With repeating the LBL cycle of coating the negatively charged CCG/P3TOPS sheets and the positively charged P3TOPA, the CCG sheets start to overlap (Fig. S3d-g), forming a continuous CCG phase in the CCG/P3TOPS-P3TOPA composite films. According to previous report,[11] both the CCG sheets and the polythiophenes are capable of forming continuous phases in the composite films prepared by LBL assembly method.

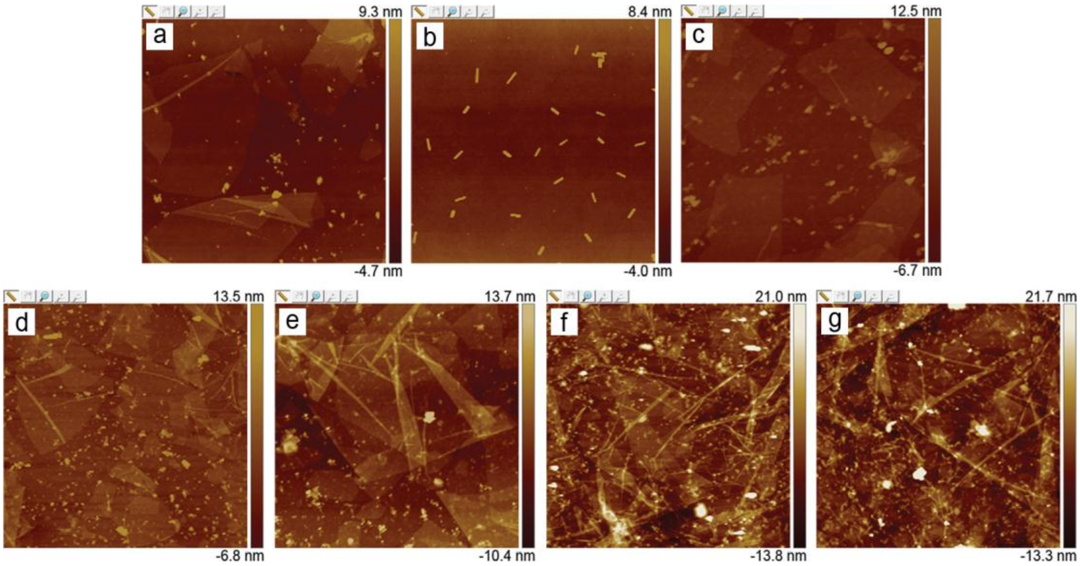

Figure S3. AFM images of (a) CCG/P3TOPS sheets coated on glass substrate by dip coating, (b) needle-like microcrystals of P3TOPA coated on glass substrate by dip coating, (c-g) 1-, 3-, 6-, 10-, and 15-cycled CCG/P3TOPS-P3TOPA composite films.

S5. I-V curves of CCG/P3TOPS-P3TOPA composite films

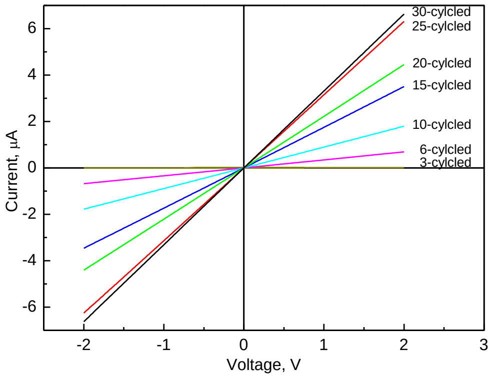

Figure S4. I-V curves of the x-cycled CCG/P3TOPS-P3TOPA composite films measured in the dark.

S6. HOMO and LUMO levels of P3TOPS and P3TOPA

The HOMO levels of P3TOPS and P3TOPA were obtained from electrochemical characterization.[12] Electrochemical characterization was done on a ZAHNER ZENNIUM electrochemical workstation in acetonitrile/DI water (95:5 in volume),[2] containing tetrabutylammonium hexafluorophosphate (0.1 M) as the supporting electrolyte, using glassy carbon as working electrode, Pt as counter electrode, and Ag/Ag^+ as reference electrode. From the onset oxidation potentials (E_{ox}) of the polymers, HOMO level was calculated according to the following equation:

$$\text{HOMO} = -e(E_{\text{ox}} + 4.71)\ (\text{eV})$$

where the units of E_{ox} and E_{red} are V vs Ag/Ag+. The bandgaps between the HOMO and LUMO levels were estimated from the UV-visble spectra. The LUMO levels of P3TOPS and P3TOPA were calculated from the data obtained above. In Fig. S5 are displayed the cyclic voltammogram (CV) curves of P3TOPS and P3TOPA. In Fig. S6 are displayed the UV-visible spectra of P3TOPS and P3TOPA. The HOMO and LUMO levels, and the bandgaps of

P3TOPS and P3TOPA are summerized in Table S1. The values of P3TOPS obtained in this study are in agreement with those reported before.[13]

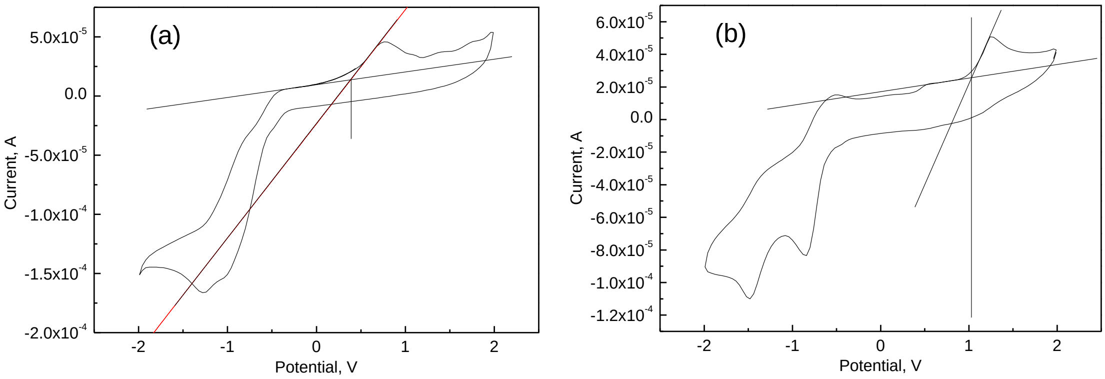

Figure S5. CV curves of (a) P3TOPS and (b) P3TOPA.

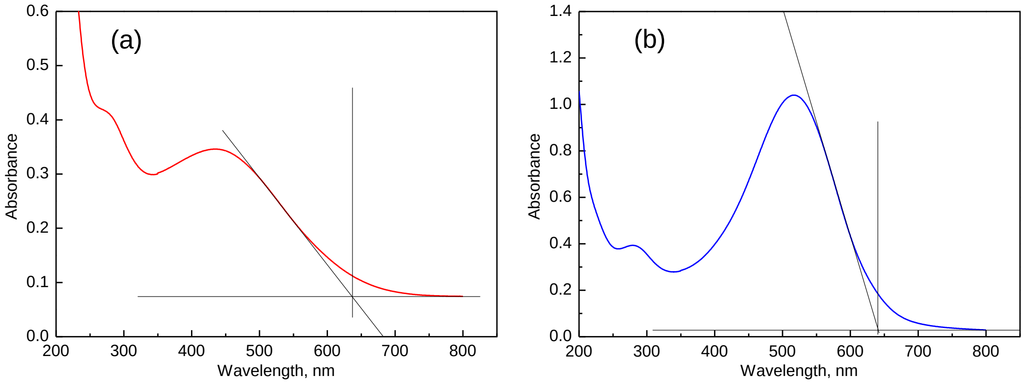

Figure S6. UV-visible spectra of (a) P3TOPS and (b) P3TOPA.

Table S1. HOMO and LUMO levels, and bandgaps of P3TOPS and P3TOPA.

	HOMO (eV)	LUMO (eV)	Bandgap (eV)
P3TOPS	-5.10	-3.15	1.95
P3TOPA	-5.74	-3.81	1.93

S7. PL spectra of CCG/P3TOPS-P3TOPA composite films

In Fig. S7 are displayed the PL spectra of P3TOPA film and CCG/P3TOPS-P3TOPA composite film. A P3TOPA film shows a PL spectrum containing an emission maximum at 577 nm when excited with a wavelength of 517 nm, the wavelength of the absorption maximum of P3TOPA. Such emission of P3TOPA is attributed to the radiative transition of the electrons from the LUMO to HOMO. In contrast, a CCG/P3TOPS-P3TOPA composite film shows a PL spectrum containing a reduced emission peak. This result is due to the electron transfer from the LUMO of P3TOPA to the Fermi level of CCG.

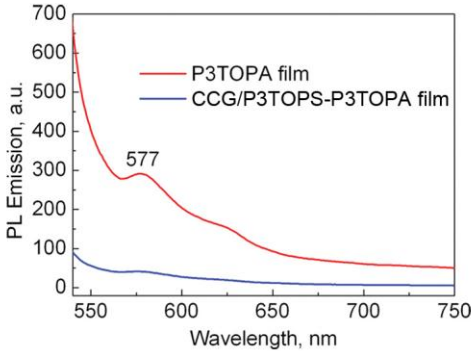

Figure S7. PL spectra of a P3TOPA film and a 25-cycled CCG/P3TOPS-P3TOPA composite film.

S8. Photosensitivity of a neat CCG film

In order to confirm that the photoinduced electron transfer from the conjugated polymers to CCG sheets plays a critical role in achieving the photoresponse properties, a CCG film that has similar thickness to a 30-cycled CCG/P3TOPS-P3TOPA composite film was used to fabricate a photoresponse device. The CCG film was prepared by filtration method.[5] The photoresponse device made of the CCG film only gives a photosensitivity as low as 1.33 % (Fig. S8).

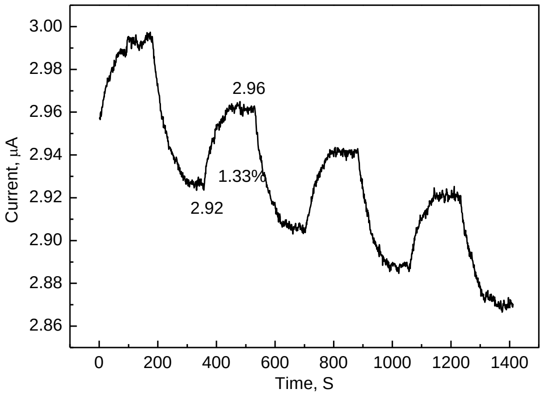

Figure S8. The current of a photoresponse device made of CCG film as the illumination path was opened and chopped.

S9. Fitting of photocurrent growth and photocurrent decay

Both photocurrent growth and photocurrent decay were fitted using monoexponential and biexponential equations, as shown below:

$$I(t) = I_{\text{dark}} + A\exp(-\frac{t}{\tau})$$

$$I(t) = I_{\text{dark}} + A\exp(-\frac{t}{\tau_1}) + B\exp(-\frac{t}{\tau_2})$$

where I_{dark} is the dark current, τ, τ_1 and τ_2 are the time constant, and A and B are the scaling constant. The monoexponential fitting and the biexponential fitting of the photocurrent growth and photocurrent decay are shown in Fig. S9 and S10. It is seen that the biexponential fitting yields better results than the monoexponential fitting for the photocurent growth (Fig. S9). In contrast, for the photocurrent decay, the monoexpoential fitting and the biexponential fitting give the same results (Fig. S10). These results demonstrate that a biexponetial equation is applicable to the photocurrent growth, and a monoexponential equation is applicable to the photocurrent decay.

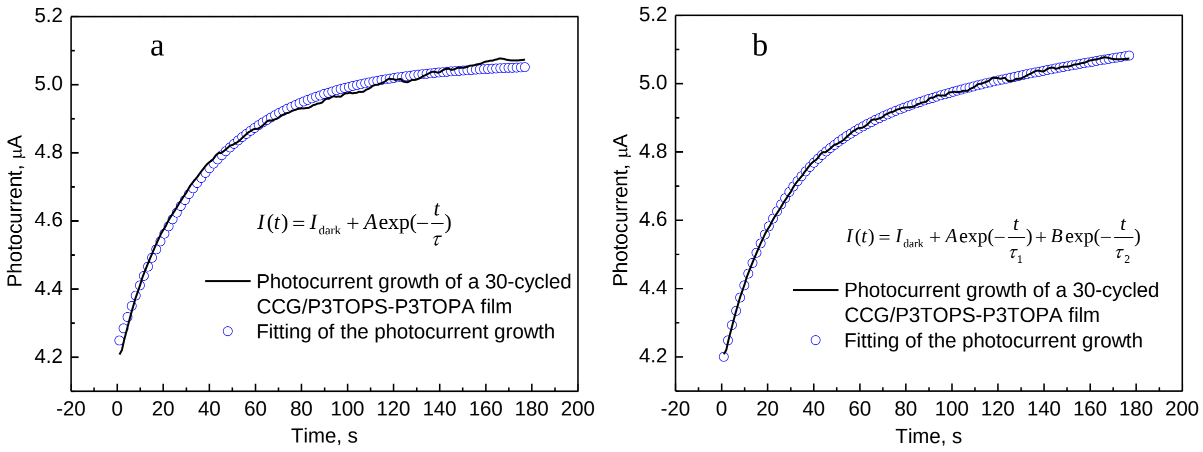

Figure S9. (a) Monoexponential fitting, and (b) biexponential fitting of photocurrent growth.

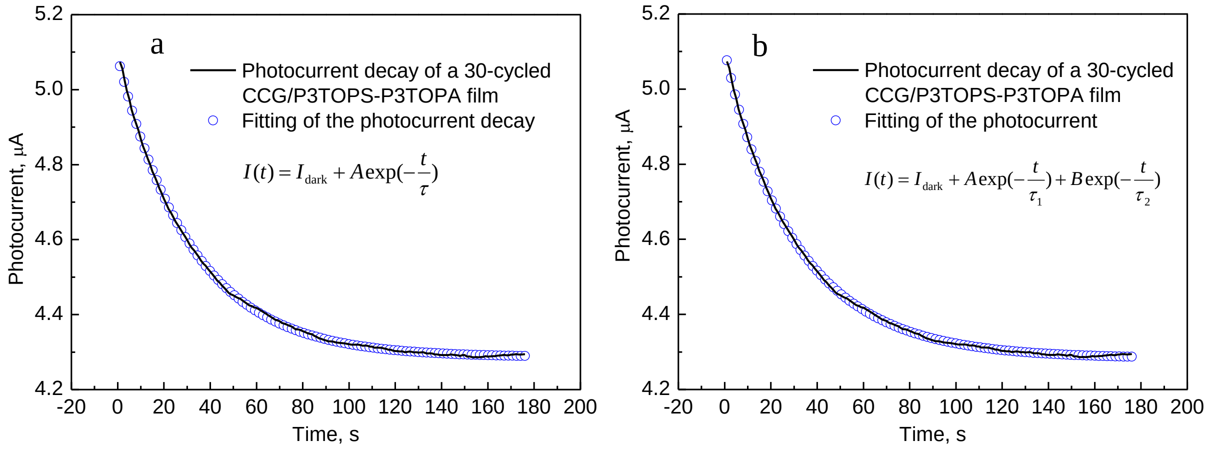

Figure S10. (a) Monoexponential fitting, and (b) biexponential fitting of photocurrent decay.

References:

1 C. Li, M. Numata, A. H. Bae, K. Sakurai and S. Shinkai, *J. Am. Chem. Soc.*, 2005, **127**, 4548-4549.

2 M. Chayer, K. Faid and M. Leclerc, *Chem. Mater.*, 1997, **9**, 2902-2905.

3 D. Li, M. B. Muller, S. Gilje, R. B. Kaner and G. G. Wallace, *Nat. Nanotechnol.*, 2008, **3**, 101-105.

4 J. Geng and H. Jung, *J. Phys. Chem. C*, 2010, **114**, 8227-8234.

5 J. X. Geng, L. J. Liu, S. B. Yang, S. C. Youn, D. W. Kim, J. S. Lee, J. K. Choi and H. T. Jung, *J. Phys. Chem. C*, 2010, **114**, 14433-14440.

6 K. Masuda, T. Abe, H. Benten, H. Ohkita and S. Ito, *Langmuir*, 2010, **26**, 13472-13478.

7 A. R. G. Smith, J. L. Ruggles, A. Yu and I. R. Gentle, *Langmuir*, 2009, **25**, 9873-9878.

8 S. Q. Liu, D. G. Kurth, B. Bredenkotter and D. Volkmer, *J. Am. Chem. Soc.*, 2002, **124**, 12279-12287.

9 X. Xiao, Z. Hu, Z. Wang and T. He, *J. Phys. Chem. B*, 2009, **113**, 14604-14610.

10 X. Xiao, Z. Wang, Z. Hu and T. He, *J. Phys. Chem. B*, 2010, **114**, 7452-7460.

11 J. Lukkari, M. Salomaki, A. Viinikanoja, T. Aaritalo, J. Paukkunen, N. Kocharova and J. Kankare, *J. Am. Chem. Soc.*, 2001, **123**, 6083-6091.

12 J. H. Hou, L. J. Huo, C. He, C. H. Yang and Y. F. Li, *Macromolecules*, 2006, **39**, 594-603.

13 Q. Q. Qiao, L. Y. Su, J. Beck and J. T. McLeskey, *J. Appl. Phys.*, 2005, **98**, 094906.